International Journal of Current Advanced Research
ISSN: O: 2319-6475, ISSN: P: 2319-6505, Impact Factor: 6.614
Available Online at www.journalijcar.org
Volume 7; Issue 5(L); May 2018; Page No. 13015-13024
DOI: http://dx.doi.org/10.24327/ijcar.2018.13024.2310

Research Article

EFFECTS OF PHOSPHORUS AND COBALT CO-DOPED ANATASE TITANIA ON THE DEGRADATION OF ORANGE II AND ANTIBACTERIAL ACTIVITY OF *STAPHYLOCOCCUS AUREUS & SALMONELLA TYPHI* IN VISIBLE LIGHT

Mulupuri Ravi Kumar., Tirukkovalluri Siva Rao*., Imandi Manga Raju., Shaik Abdul Alim and K.V. Divya Lakshmi

Department of Inorganic & Analytical Chemistry, School of Chemistry, Andhra University, Visakhapatnam, Andhra Pradesh-530003, India

A R T I C L E I N F O

Article History:

Received 24th February, 2018
Received in revised form 19th March, 2018 Accepted 16th April, 2018
Published online 28th May, 2018

Key words:

Photocatalysis; Sol-gel method; Orange II; co-doping; Phosphorus and Cobalt; *Staphylococcus aureus* and *Salmonella typhi.*

A B S T R A C T

The increasing demand for water and declining supply has made the photocatalytic treatment and recycle of industrial effluents an attractive option. The discharge of orange II (azo-dye) into the environment causes water pollution due to its colour, toxicity, mutagenicity and carcinogenicity. Phosphorus and cobalt codoped TiO_2 nanomaterial was successfully prepared by single step sol–gel method by doping different weight percentages of dopants concentrations into TiO_2 lattice. The co-doped TiO_2 samples were characterized to confirm the structural and morphological changes in TiO_2 crystal lattice by using X-ray Diffraction (XRD), Scanning Electron Microscopy (SEM), Energy Dispersive X-ray (EDX), Transmission Electron Microscopy (TEM), UV-Visible Diffuse Reflectance Spectroscopy (UV-vis.DRS), X-ray Photo electron spectroscopy (XPS), Brunauer-Emmmett-Teller surface area analyzer (BET) and Fourier Transform Infrared Spectroscopy (FT-IR). The characterization results revealed that all the codoped samples show anatase phase, nanoparticle (5.8nm) and narrow band gap(2.54eV). These results enhances the photocatylytic activity of co-doped anatase titania in visible light for the degradation of orange II dye with in 35 min and antibacterial activity on *Staphylococcus aureus* & *Salmonella typhi* in 180 min.

INTRODUCTION

This paper investigates the effects of photocatalytic degradation and anti bacterial activity by P, Co codoped TiO_2 azo dye i.e orange II and also its antibacterial activity. Every procedure has its own limitations for waste water treatment, but among all the semiconductors nano sized titania in anatase form was the more promising semiconducting material for environmental applications due to its high photo-reactivity (Ya *et al*., 2007; Zheng *et al*., 2010) chemical stability, good durability in hostile environments, bio-compatibility, water insolubility and non photo corrosive nature, but photoactive in ultrviolet region. To obtain the visible light active anatase TiO_2 many attempts has been made to get visible light activity by doping with metals (Cantau *et al*., 2010; Wu *et al* .,2009; Ohno *et al*., 2004; Lv *et al*., 2009; Huang *et al*., 2007) non-metal (Choi *et al*., 1994; Wu *et al*., 2004; Liu *et al*., 2011; Zhao *et al*., 2008; Cantau *et al*., 2010; Wu *et al*., 2009; Ohno *et al*., 2004; Lv *et al*., 2009) and co-doping with metal-metal and metal-nonmetals.

Corresponding author:* **Tirukkovalluri Siva Rao
Department of Inorganic & Analytical Chemistry, School of Chemistry, Andhra University, Visakhapatnam, Andhra Pradesh-530003, India

Among these co-doping combinatios metal-nonmetal co-doping improved the photocatalytic activity of antase titania in visible light due to enhancing the electron–hole pairs separation, reduced electron recombination processes, decrease in grain size and active under visible light irradiation. According to literature survey, among non-metals, phosphorus (P) doping (Shi *et al*., 2006) is found to be most photocatalytic activity of TiO_2 due to increase in the surface area and stabilizing anatase (Yu *et al*., 2003; Fan *et al*., 2008; Yu *et al*., 2010; Yu *et al*., 2010) structure. Where as in metals cobalt (Co) doping decreases the electron-hole pair recombination rate and acts as electron trap (Choi *et al*., 1994; Wang *et al*., 2009) enhances the photocatalytic activity (Lin *et al*., 2007). Hence, in the present investigation phosphorus (P) and cobalt (Co) have been selected for the synthesis of P,Co co-doped TiO_2 nanomaterial by using sol-gel method and antibacterial activities of the phosphorus (P) and cobalt(Co)co-doped TiO_2 were investigated by the cup plate method or agar-well diffusion method evaluated on the surface of Mueller Hinton agar plates, gentamicin (200µg/mL), vancomycin (1µg/mL) and fluconazole (25 µg/mL) were used as reference antibiotics. Photocatalytic action and photocatalysis on microorganisms has been shown to be capable of killing a wide range of organisms including gram-negative and gram-positive bacteria

(Staphylococcus aureus and Salmonella typhi) (Paspaltsis *et al*. 2006). Photocatalysis has also been shown to destroy microbial toxins. Several studies indicates that metal-non-metal co-doped TiO_2 may attach to the surface of the cell membrane disturbing permeability and respiration functions of the cell. Among all the methods available, sol-gel method is advantageous because homogeneity, high purity, low temperature and stoichiometric control than precipitation, (Kapusuz *et al*., 2013) hydrothermal, (Kim *et al*., 2008) chemicalvapour deposition, (Zang *et al*., 201) electcosprining, (Putz *et al*., 2017) and so on. The photocatalytic activity of as prepared catalyst was verified by the degradation of orange II dye. Azo dyes (orange II) are generally resistant to biodegradation due to their complex structures. Orange II is one of the most widely used dyes in the textile industry orange II dye is a non-biodegradable and mutagenic in nature. Thus orange II dye has been widely used in textile industry. To minimize the orange II pollution in the environment many researchers have been under taken various methods (Mittal *et al*., 2009) to degrade.

Experimental

Materials required

Titanium tetra-n-butoxide(E-Merk ,Germany), Triethyl phosphate (E-Merk, Germany), cobalt(II)nitrate (Sigma Aldrich) were used as precursors for Ti, P, and Co respectively. All the chemicals used in the synthesis process were reagent grade and the solutions are prepared in double distilled water without further purification. Mueller Hinton agar medium to be used for routine susceptibility testing of bacteria due to its acceptable reproducibility, satisfactory growth of most pathogens. Sabouraud's dextrose agar was used for susceptibility testing of fungi.

Synthesis of Phosphorus, Cobalt co-doped TiO_2 nanomaterial

Phosphorus and cobalt codoped TiO_2 samples were prepared by varying the dopant concentrations with respect to amount of TiO_2.

Preparation procedure

15 mL of Titanium tetra-n-butoxide along with 30 mL of absolute ethanol taken in a 150 mL pyrex glass beaker and stirred for 10min. 2.1mL of HNO_3 was added drop wise to this solution and continue the stirring up to 30 min. This solution was further considered as solution I. In another beaker 30 mL of absolute ethanol and 4.32 mL of H_2O along with the dopants i.e triethyl phosphate and cobalt nitrate were taken as per the required amounts of dopants with respect to TiO_2 (solution II) and stirred the solution for 30 min. Solution II was added to solution I from the burette slowly under continuous vigorous stirring at room temperature until the transparent sol was formed and again continue the stirring for 2 hrs at room temperature. The sol obtained was kept in dark for 48 hrs to ageing for gel formation. The gel was dried in an oven at 100 ^{0}C and ground. The catalyst powder was calcined at 450 ^{0}C in a muffle furnace for 5hrs; cool the catalyst powder to room temperature and ground. The same procedure was adopted for the preparation of undoped TiO_2 without addition of dopants.

Table.1 Name assigned to different weight percentage of TiO_2 co-doped catalysts

S.N	Code name of the samples	Wt% of dopants doped into TiO_2	
		Phosphorus	Cobalt
01	PCT_1	0.75 w%	0.25 w%
02	PCT_2	1.0 w%	0.25 w%
03	PCT_3	0.50 w%	0.50 w%
04	PCT_4	0.25 w%	0.75 w%
05	PCT_5	0.25 w%	0.25 w%
06	PURE TiO_2		

All the catalysts samples and undoped samples prepared were given code numbers and tabulated in the Table.1.

Instrumental techniques used for the Characterization of catalysts

The synthesized photocatalysts were characterized by various sophisticated analytical Techniques. UV-vis DRS Spectra are taken by using Shimadzu 3600 UV-vis & DRS NIR Spectrophotometer with an integrating sphere diffuse reflectance is used. XRD patterns of the samples were recorded by using Ultima IV, RIGAKU model with anode Cu-WL1 λ=1.5406nm, nickel filter-current-40 mA, voltage-40 kV, with 2θ scanning range 5.000-90.9505, scan rate of 10.1600 s^{-1}. XPS was recorded with a PHI quantum ESCA microprobe system, using the ALKα line of a 250w X-ray tube as a radiation source with the energy of 1253.6 eV, 16 mA × 12.5 kV and working under the pressure lower than $1\times10^{-8}Nm^{-2}$. Morphology and size of the anatase particles was determined by SEM model JSM-6610 LV equipped with an energy dispersive X-ray (EDS) voltage 20 kV. BET is a used to determine pore size, pore volume and surface area of anatase particles from N_2 adsorption desorption isotherm at 77.3 K, model-NOVA 2200E system. TEM was determined by model TECNAI FE12 TEM operated at voltage-120 kV. FT-IR spectra were recorded by using FT-IR spectrometer model-Nicolot Avatar-360. orange II degradation was monitored by using UV-vis spectrophotometer model - Shimadzu 1601.

Photocatalytic activity measurements

The high pressure mercury metal halide lamp (400 W) with UV filters oriel no: 51472 was placed 20 cm away from the reaction mixture. To remove IR radiation source and to keep the reaction mixture at room temperature the running cool water was circulated around the sample container. The photocatalytic procedure was carried out with a required amount of catalyst dosage added to fresh 100 mL of aqueous dye solution containing 10 mgL^{-1} dye taken in a pyrex glass vessel with continues starring. Prior to irradiation the solution was adjusted to required pH by the addition of either 0.1N HCl or 0.1N NaOH. The solution was continued the starring for 30 min in dark to achieve the adsorption and desorption equilibrium between dye and catalyst surface and then exposed to visible light. Then 5 mL aliquots of samples were withdrawn from the reaction mixture by using millipore syringe (0.45μm) at different time interval and measure the absorption of the sample at λ_{max} 620 nm by using UV-VIS spectrophotometer (Milton Roy Spectonic 1201). The percentage of degradation of the dye (orange II) was calculated by using the following equation.

$$\% \text{ of Degradation} = A_o\text{-}A_t / A_o \times 100,$$

where A_o is initial absorbance of dye solution before exposure to light and A_t is absorbance of dye solution at time t after exposure to light.

RESULTS & DISCUSSIONS

X-Ray Diffraction Studies (XRD)

The powder X-ray diffraction patterns of undoped and co-doped phosphorus and cobalt TiO_2 were recorded in Fig.1 (a) & (b) at $2\theta = 20^0$ to 80^0. For all the undoped and co-doped samples the maximum peak were observed at $2\theta = 25.14^0$ indicated that the formation of anatase phase (JCPDS NO:21-1272) (Gomathi *et al*., 2010). The other peaks were observed at 2θ of 37.83^0, 47.88^0, 54.87^O,74.83^0 and 82.56^0 with indices corresponding to (004), (200), (211),(215),(224) planes respectively and also coincide with that of undoped TiO_2 indicates that co-doping did not influence the anatase phase of TiO_2. There are no characteristic peaks were observed for phosphorus and cobalt oxides in XRD spectrum in all the codoped samples, which indicates that the phosphorus and cobalt ions are incorporated into the lattice of anatase TiO_2 in place of Ti^{4+} ion. According to the FWHM analysis of the anatase diffraction peak and based on the scherrer formula (Meshesha *et al*., 2017) the average crystallite size of undoped and co-doped TiO_2 samples were found to be 36.8 nm & 5.7 nm-12.1 nm. From these results decrease in crystallite size was observed due to co-doping of cobalt and phosphorus into TiO_2 lattice. The variation in the particle size and the phase content demonstrated that P doping decreases the particle size, aggravate the unit cell distortion, retards the phase transformation of anatase to rutile (Neeruganti *et al*., 2012) and the reducing atmosphere due to P-doping was more efficient in slowing down the crystal-growth rate in P,Co co-doped TiO_2 (Ma and Guo,2011; Yu and Yu, 2007). The comparative results of pure TiO_2, single doped, Phosphorus and cobalt co-doped crystallite size with co-doped TiO_2 are given in the Table.2. The results from Table.2 confirm that the P,Co co-doped samples having less crystallite size compared to that of phosphorus and cobalt single doped TiO_2 samples in which PCT_1 show less crystallite size (8.1nm).

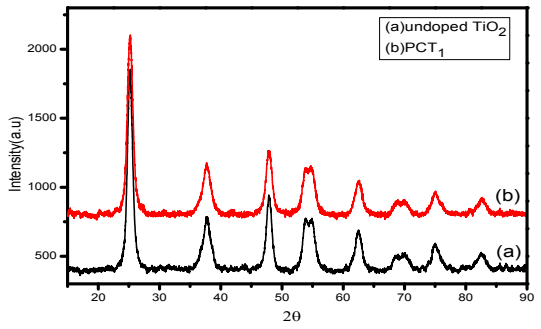

Fig 1 XRD pattern of the synthesized undoped and co-doped TiO_2 with 0.75wt% of P & 0.25wt% of Co.

Table 2

S.No	Catalyst code	Band gap eV	Crystallite size nm
01	Undoped TiO_2 (T)	3.14	36.8
02	P-doped TiO_2 (PT)	3.1	10.8
03	Co-doped TiO_2 (CT)	3.65	19.90
04	P,Co-codopedTiO_2 (PCT)	2.54	8.1

X-ray photo electron Spectroscopy (XPS)

X-ray photo electron Spectroscopic analysis study was carried out to confirm the presence of Ti, P, Co, O & C and analysed their chemical state. Fig. 2(a) shows the survey spectra of 0.75 wt% of P and 0.25 wt% of Co co-doped TiO_2 and their magnifying spectra of Ti, P, Co, O & C were shown in the Fig. (2b-2f). The binding energies of Ti $2p_{3/2}$ and Ti $2p_{1/2}$ Fig. 2(b) components of PCT_1 catalyst are located at 459.653ev and 465.218ev (Xia *et al*., 2014) which corresponds to Ti^{4+} ion in TiO_2 lattice. The doublet peak Fig. 2(c) of $P2p_{3/2}$ and $P2p_{1/2}$ corresponding binding energies at 134.116 eV and 135.222 eV respectively. This indicated that the presence of P^{5+} ion in TiO_2 lattice as a substitution dopant by replacing Ti^{4+} ion (Shi *et al*., 2006). This results attributed that phosphorus present as P^{5+} ion but not as PO_4^{3-} ion. As per the literature reports if phosphorus presents as phosphate ion the binding energy should appear at 133.7 eV (Chang *et al*., 2009). In the present case the binding energies appears at higher side. Hence the phosphorus cannot present as a phosphate ion. This result coincides with XRD results. This suggesting that phosphorus in pentavalent oxidation state ascribing the existence of Ti-O-P bonds. It is important to note that no Ti-P bond is present since no peak was observed at 129 eV where P atom replaces O atom in TiO_2 crystalline lattice (Yu *et al*., 2010). The replacement of Ti^{4+} by P^{5+} caused a charge imbalance has been compensate this effect, by reducing the number of oxygen vacancies resulting in the enhancement of the photo catalytic activity (Yu *et al*., 2005). The doublet peak in Fig. 2(d) of cobalt $2p_{3/2}$ and cobalt $2p_{1/2}$ peaks are located at binding energies of 782.52 eV and 801.448 eV, respectively, which indicated that, a shift towards positive value due to phosphorus doping. These peaks confirms the presence of cobalt in TiO_2 lattice as Co^{2+} oxidation state as a substitution dopant occupying the Ti^{4+} site in TiO_2 lattice (Barakat *et al*., 2005; Mungundan *et al*., 2015). From the Fig. 2(e) 1s spectrum of oxygen shows two peaks at 530.646 eV & 532.554 eV and a strong peak at 530.646 eV is attributed to lattice oxygen in Ti-O bond and a small peak at 532.554 eV corresponding to adsorbed oxygen species such as O and OH groups on the surface of TiO_2 codoped catalyst (Meshesha *et al*., 2017).

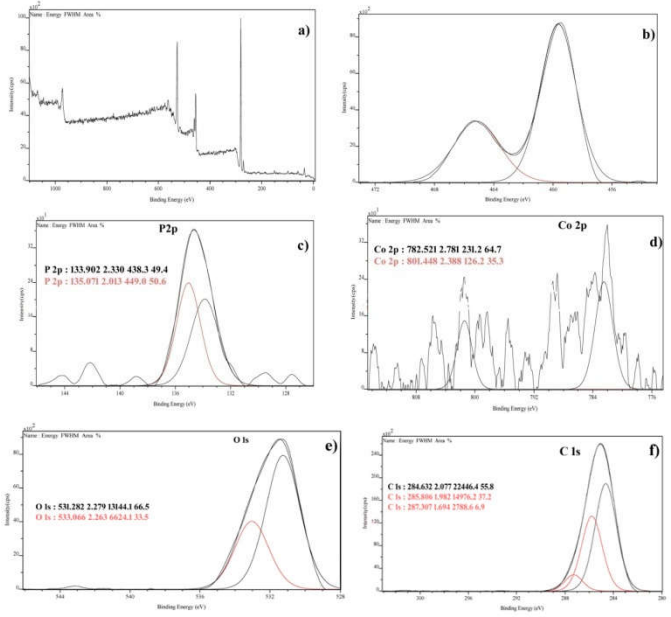

Fig 2 a) XPS survey spectrum of co-doped TiO_2 and high resolution spectrum of (b) Ti 2p (c) P 2p (d) Co 1s (e) O1s (f) C1s

Fourier Transform-Infra Red Spectroscopy (FT-IR)

The FT-IR spectra of undoped and P, Co codoped TiO_2 (PCT_1) nanomaterials illustrated that the peaks at 3474 cm^{-1} & 1647 cm^{-1} corresponding to stretching and bending vibrations of O-H (Najibi *et al*., 2006) and H-O-H (Singla *et al*., 2014) of both the catalysts (undoped and co-doped) respectively. The stretching frequency band at 512 cm^{-1} corresponding to Ti-O-Ti network which coincides with literature value (Elmorsi *et al*., 2010; Sharopri and Sud, 2015). This band shifted to 567 cm^{-1} in the codoped samples. Due to codoping, the Ti-O-Ti network was destroyed, a new peaks are arises at 549 cm^{-1} & 679 cm^{-1} which are attributed to the formation of Ti-O-P or Ti-O-Co or Co-O-P (Susmitha *et al*., 2014). This can also be explained in terms of new interactions of dopants causes deformation in octahedral symmetry of Ti^{4+} in TiO_2 lattice (Yu *et al*., 2003).

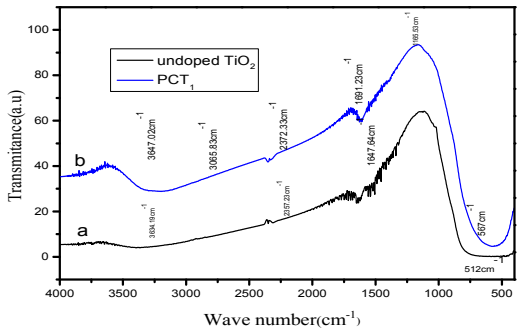

Fig 3 FT-IR spectra of (a) undoped TiO_2 and (b) 0.75 wt% of P & 0.25 wt% of Co co-doped TiO_2 (PCT_1).

Ultra violet-Visible Diffuse Reflectance Spectroscopic Studies (UV-Vis.DRS)

UV-Vis.DRS spectra of undoped and co-doped TiO_2 samples were given in Fig .4(a). It is observed that the co-doped samples have a profound effect on its optical response in the visible wavelength range. Compared to undoped TiO_2 the extension of absorption edge towards longer wavelength (red shift) for co-doped samples indicated the decrease in band gap. This is may be due to the formation of an extra energy level above the valance band by P_{2p} and O_{2p} states in co-doped TiO_2 samples. Further it was supported by the calculated band gap energies of the all synthesized samples from the reflectance spectra using the Kubelka-Monk formalism and Tauc plot method (Rauf *et al*., 2011) as shown in Fig. 4(b). The undoped TiO_2 exhibited the band gap of 3.14 eV which is comparable with the literature value (Yoong *et al*., 2009) and the co-doped TiO_2 samples showing the band gap ranging from 2.54 to 2.67 eV. Among all the co-doped samples PCT_1 exhibiting less band gap energy i.e 2.54 eV. Cobalt doping forms extra energy level between within the band gap and acts as electron-trap centre and enhances electron-holes pairs separation leads to increase in photocatalytic activity of co-doped samples PCT_1. Thus the results indicated that all the co-doped samples are visible light active leads to better photocatalytic degradation efficiency by formation of photo generated electron/hole pairs.

The DRS spectra of undoped TiO_2 and co-doped TiO_2 with 0.75 wt% of P & 0.25 wt% of Co (b) Tauc plots of the square root of the Kubelka-Munk function $(F(R)hv)^{1/2}$ vs photon energy(hv) for determining bandgap energy values.

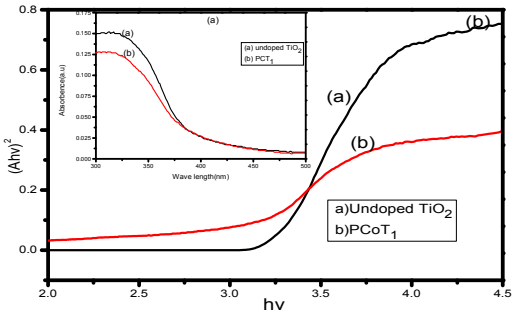

Fig 4 (a) UV-vis absorption spectra of as prepared samples (b) Tauc Plot

Scanning Electron Microscopy - Energy Dispersive X-ray (SEM-EDX)

Fig.5(a) & 5(b) shows typical scanning electron microscopic images of undoped and 0.75wt% of P & 0.25wt% of Co co-doped TiO_2(PCT_1) indicated these particles are in spherical shape, smooth surface and little agglomeration. From the SEM results it can be concluded that agglomeration and particle sizes are decreased (Yu anad Yu,2007) greatly in PCT_1 due to codoping of P and Co into TiO_2 lattice and their presence was confirmed by EDX analysis Fig.5(d).

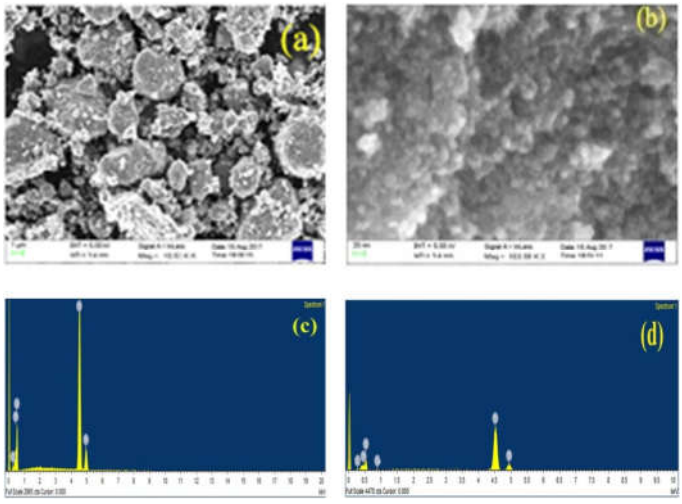

Fig 5 The SEM images of (a) undoped TiO_2 (b) PCT_1 and the EDS (c) undoped TiO_2 and (d) PCT_1.

Transmission Electron Microscopy (TEM)

TEM images of undoped and co-doped TiO_2 samples are given in Fig.6(a) & 6(b). In these images it is observed that codoped TiO_2 samples show less particle size than that of undoped TiO_2. Fig.6(c) depicted the selected area electron diffraction (SEAD) pattern of the PCT_1 , clearly indicated the defined concentric rings which were obtained due to the diffraction from the (101), (004), (200), (211) planes of the anatase TiO_2. The average particle size of undoped and codoped samples were caliculated by the Guassian fitting of the size histogram as shown in the Fig. 6(e) and found to be 4.8 nm. These results strongly confirmed that, the co-doping of P and Co in TiO_2 lattice decreased the particle size. These results strongly confirmed that, the co-doping of P and Co in TiO_2 lattice decreased the particle size.

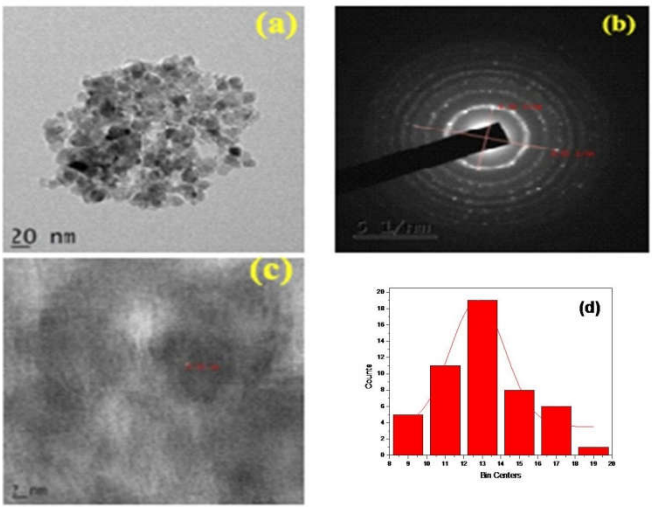

Fig 6 TEM images of (a) 0.75 wt% of P & 0.25 wt% of Co co-doped TiO_2, (b) SAED pattern (c) HRTEM image and (d) Histogram showing particle distribution of 0.75 wt% of P & 0.25 wt% of Co co-doped TiO_2.

BET – Surface area analysis

Brauner-Emmett-teller (BET)

Accordingly, the BET specific surface area for prepared five samples show an increase than the undoped TiO_2 indicates microspore which in turn provides highest photocatalytic activity for PCT_1 towards orange-11 dye. The results of BET surface area, pore volume and pore size for the synthesized catalysts were presented in Table.3 and it is inferred that PCT_1 is a mesoporous material showing type IV isotherm. Among all the co-doped samples PCT_1 shows high surface area with 9.8549 m^2/g, pore volumes 0.11567cm^3/g and pore size 50.92 A^0. These values are higher than non-porous TiO_2 material. Our findings clearly indicates that P,Co co-doped TiO_2 have a larger surface area and greater N_2 adsorption capacity than pure TiO_2, which is due to the increase in the pore size.

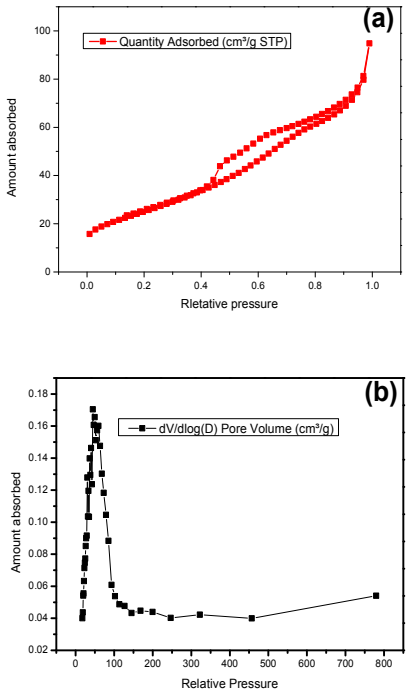

Fig 7 (a)&(b) BET isotherm data revealing the mesoporus nature of the P,Co codoped TiO_2 sample PCT_1.

Photocatalytic activity evaluation of PCT_1 by the catalyst degradation of Orange II dye

Degradation of Orange II dye (O-II)

In order to measure the photocatalytic efficiency of synthesized nano catalyst PCT_1 the experiments were carried out by varying the reaction parameters such as effect of dopant concentration, initial pH, catalyst dosage and initial dye concentration. Initially blank experiments were performed with dye in presence and absence of visible light and another reaction along with synthesized nano catalyst in presence and absence of visible light and another reaction along with synthesized nano catalyst in presence and absence of light were performed. In both the reactions there is no significant degradation was observed. But in the second reaction a complete degradation was observed without visible light in both the cases. But in the second case reaction a complete degradation was observed in visible light. This clearly demonstrated that for photocatalytic degradation of orange-II dyes both catalyst and visible light are necessary. To obtain the complete degradation of the dye there is a need to evaluate optimum conditions by studying the effects of reaction parameters.

Effect of dopant concentration

To determine the rate of photocatalytic degradation of orange II dye solution a series of experiments were conducted by using the synthesized catalysts with different dopant concentrations were presented in Fig. 8(a). All the co-doped samples have higher photocatalytic activity than undoped TiO_2 under visible light irradiation. This indicated that co-doping has improved the photo catalytic performance of TiO_2 in visible light. Among all the co-doped catalysts, PCT_1 shows highest rate to at these dopants concentrations (0.75 wt% of P & 0.25 wt% of Co) there is an increase in number of trapped charge carriers per particle (Kapusuz *et al*., 2011). Further increase in dopant concentration the rate decreases, this is may be attributed that the average distance between trap sites decreases with increasing the number of dopants confined within a particle (Choi *et al*., 1998).

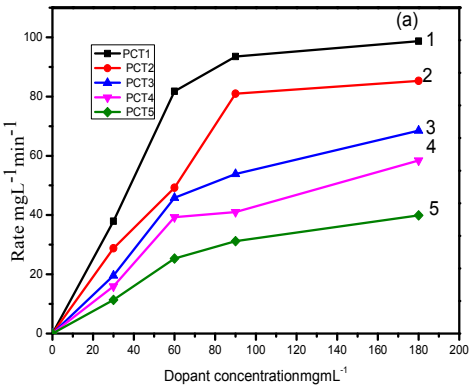

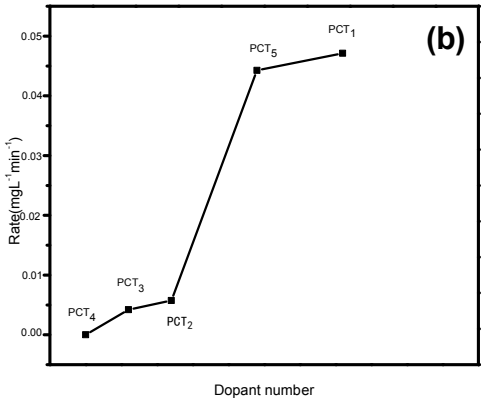

Figure 8(a)&(b). The effect of dopant concentration on photocatalytic activity of co-doped titania by degradation of Orange II. Here, catalyst dosage 10 mgL^{-1}, pH 2 and [Orange II] 5 mgL^{-1}.

Effect of pH

pH is proposed to be a major factor influencing the rate of photocatalytic performance (Lachheb *et al*., 2002) of the catalyst. To understand the effect of pH, experiments were carried out by varying the pH from 1 to 8 by kept the other parameters constant and the experimental results are presented in the Fig. 9(a)&(b). The results indicated that the rate of degradation increases with increase of pH up to 2, later this rate decreases. When the pH is less than 2, the degradation of orange-II slowly increases, it may be due to the increase in the production of $OH^{\bullet}$ radicals and their existence leads to competition between dye negative(-ve) molecules and $OH^{\bullet}$ radicals. Further the rate will be increased as $OH^{\bullet}$ radicals consumption increase for the degradation of adsorbed dye molecules. In acidic pH the percentage of degradation of orange II was found to be high at pH 2, at which the positive charge (H^{+} ions) on TiO_2 surface increases and negatively charged dye molecules can easily adsorbed its surface, which leads to high percentage of degradation of dye. When the pH increased to basic medium the catalyst surface changes to negative and electrostatic repulsion with the same charge on the dye molecules, which causes a decrease in the rate of degradation as shown in the Fig. 9(a)&(b). The rate of degradation of orange-II increases up to pH 2 further rate slowly decreases as H^{+} ions decreases. This influences the diminishing of +ve charge of the catalyst surface slowly when the pH going towards the high pH then, the rate of degradation decreases.

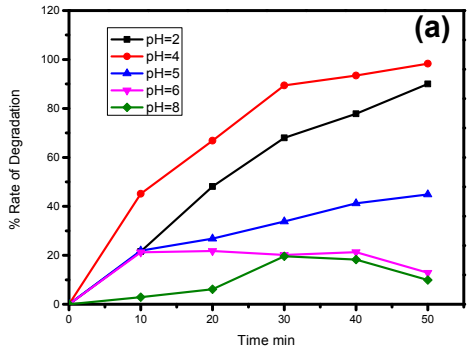

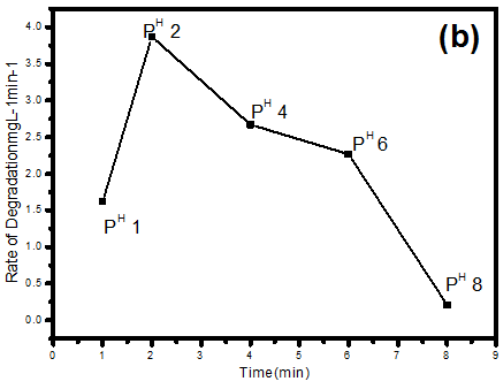

Figure.9 (a)&(b). The effect of pH on the rate of degradation of by Orange II 0.75 wt% of P & 0.25 wt% of Co co-doped TiO_2. Here, catalyst dosage 10 mgL^{-1} and [Orange-II] 10 mgL^{-1}.

Effect of catalyst dosage

The effect of catalyst dosage on degradation of orange II has been given in Fig. 10(a)&(b). The rate of degradation of orange II was carried out by varying the catalyst amounts of 25 mgL^{-1}, 50 mgL^{-1},100 mgL^{-1}, 200 mgL^{-1} and 250 mgL^{-1} , added to 100 mL of solution containing 5mgL^{-1} of dye at p^{H} 2. The rate of degradation increases linearly with the increase of catalyst loading up to 100 mgL^{-1}, further increasing in the catalyst dosage the degradation decreases. This may be due to increase in turbidity, agglomeration of the catalyst particles which restricts the penetration of light transmission to activate the catalyst particles (Chen,2007). The collision between active catalyst particles and ground state catalyst particles of co-doped TiO_2 results in deactivation of the catalyst particles (Kusvuran *et al*., 2004). Hence the optimum catalyst dosage found to be 100 mgL^{-1}.

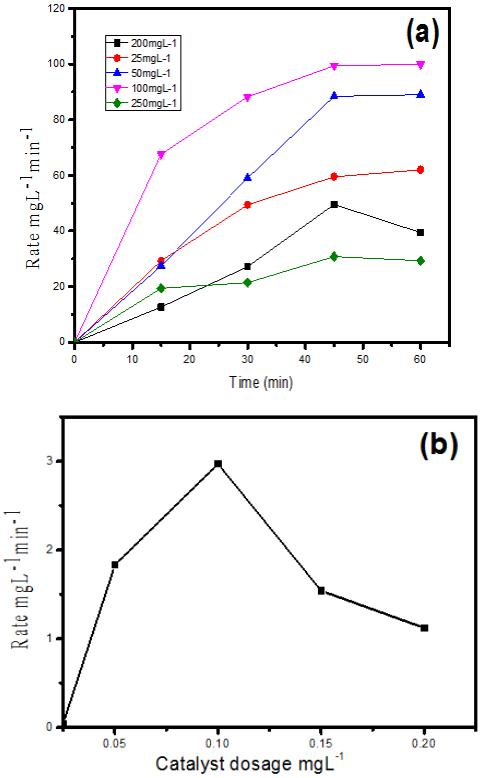

Figure 10 (a)&(b). Effect of catalyst dosage on the rate of degradation of Orange II by 0.75 wt% of P & 0.25 wt% of Co co-doped TiO_2. Here, pH 2 and [Orange II] 5 mgL^{-1}

Effect of initial concentration of dye (Orange II)

To study the effect of initial concentration of dye (orange II) at a fixed weight of catalyst 100mgL^{-1}and at pH 2, experiments were carried out with different concentrations of orange II dye from 2mgL^{-1} to 10 mgL^{-1} and results are presented in Fig. 11.(a)&(b). Results reveals that the rate of degradation of orangeII dye was very high at 5 mgL^{-1} and further increase in dye concentration causes deactivation of the catalyst due to the blanket effect (Choi and Juang, 2007).

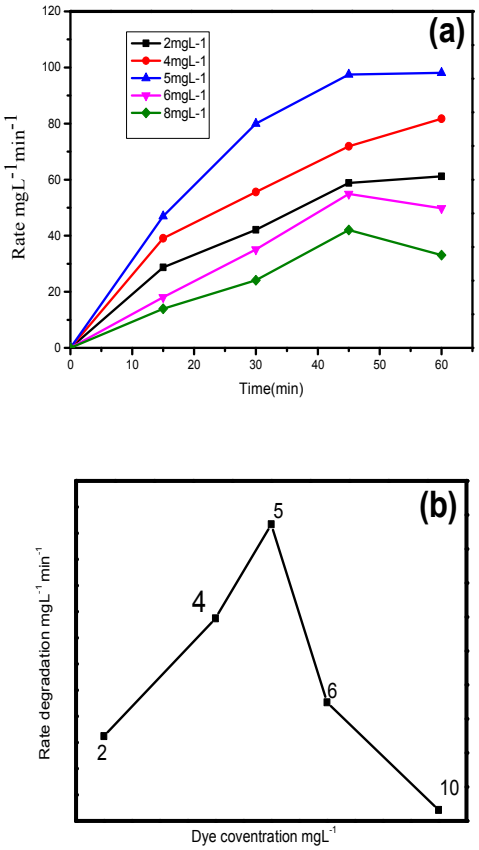

Figure11. (a)&(b) The effect of initial concentration of dye on the rate of degradation of Orange II. Here, pH 2, catalyst dosage 200 mg

Evaluation of antibacterial activity of $PCoT_1$ on Staphylococcus aureus and Salmonella typhi in visible light:

Agar-well diffusion testing

The cup plate method or agar well diffusion method depends upon diffusion of antibiotic from a vertical cylinder through a solidified agar layer in a petridish or plate to an extent such that growth of added microorganisms is prevented entirely in a zone around the cylinder containing solution of the antibiotics .The cup-plate method is simple and measurement of inhibition of microorganisms is also easy cup-plate method is simple and measurement of inhibition.

Antibacterial activities of the compounds investigated were first evaluated by agar-well diffusion method. The standardized cultures of test bacteria were first evenly spread onto the surface of Mueller Hinton agar plates using sterile cotton swabs and fungi was spread on sabouraud's dextrose agar plated using sterile cotton swabs. Five wells (6 mm diameter) were made in each plate with sterile cork borer. Fifty microliters of each of the compound and positive control was added in wells. gentamicin (200µg/mL), vancomycin (1µg/mL) and fluconazole (25µg/mL) were used as reference antibiotics. Diffusion of compounds, antibiotics and DMSO were allowed at room temperature for 1hr. All of the plates were then covered with lids and incubated at 37□C for 24hr. After incubation, plates were observed for zone of bacterial growth inhibition. The size of inhibition zones was measured and antimicrobial activity of the compounds was expressed in terms of the average diameter of inhibition zone in millimeters. Those compounds that were unable to exhibit inhibition zone (inhibition zone diameter less than 6mm) were considered non-active. Each compound was tested in triplicate with two independent experiments and mean values of inhibition zone diameters were taken. The results are shown in the Fig .10&11 and a plot showing the decrease in size of the colony with respect to time in minutes in Fig.9

Petridish

Reagents and Materials

Microorganisms

1. Staphylococcus aureus
2. Salmonella typhi

Glass ware

Petri plates 2)Test tubes 3)Spreader 4)Borer

Table 2:

Compounds used for antimicrobial studies

S. No	Compound Code
1	Undoped TiO_2
2	$PCoT_1$
3	$PCoT_3$

Positive control: **Gentamicin (10 µg)**

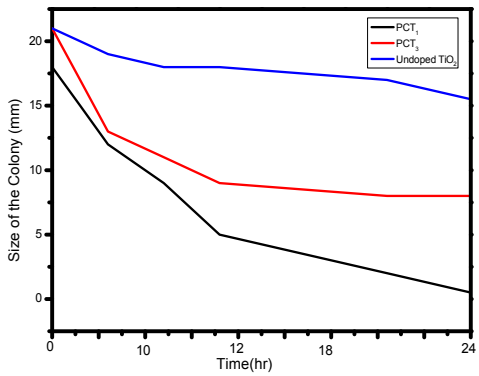

Fig 9 Graph representing the survival size of the colony in mm of bacteria Vs time of exposure to visible light of undoped, $PCoT_1$ and $PCoT_3$ codoped photocatalyst.

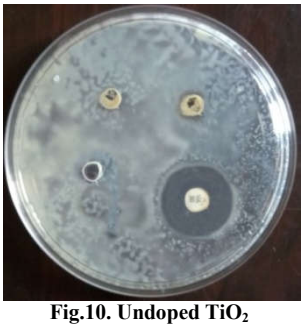

Fig.10. Undoped TiO_2

$PCoT_1$

Fig 10 Inhibition zones of four compounds *Salmonella typhi*.

Fig.11. Undoped TiO_2

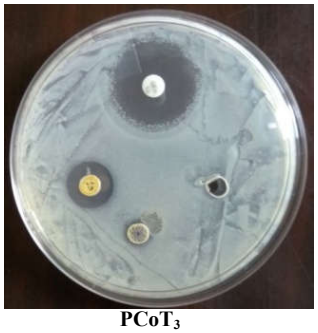

$PCoT_3$

Fig 11 Inhibition zones of four compounds *Staphylococcus aureus*

CONCLUSION

P and Co co-doped anatase TiO_2 nano catalysts with small particle size and less band gap energy were successfully synthesized by sol-gel method and characterised by various analytical techniques. In PCT_1 co-doped TiO_2, phosphorus causes the shift in absorbance band of TiO_2 from UV to visible region, whereas doping of cobalt inhibits the electron/hole recombination and acts as charge carrier during photocatalytic degradation and antibacterial activity against *Staphylococcus aureus* & *Salmonella typhi*. Under visible light irradiation PCT_1 (0.75 wt% of P and 0.25 wt% of Co) co-doped TiO_2 exhibited high photoctalytic activity compared to other nano catalysts and undoped TiO_2. Finally the optimum reaction parameters were established for complete degradation of dye orange II at $5mgL^{-1}$ dye was successfully degraded by 100 mgL^{-1} of catalyst (PCT_1) at p^H 2 under visible light irradiation for 35 min. It may be concluded that PCT_1 co-doped TiO_2 acts as better photocatalytic activity and good antibacterial agent against *Staphylococcus aureus* and *Salmonella typhi* in 24Hrs.

References

Barakat. M, Hayes. A, and Shah. G. 2005. Effect of cobalt doping on the phase transformation of TiO_2 nano particles. *Journal of Nanoscience and Nantechnology .,* 5 (5): 759-765.

Bhandari. S, Vardia. J, Malkani. K. R and Ameta. C. S. 2006. Effect of transition metal ions on photocatalytic activity of ZnO in bleaching of some dyes. *Toxicology Environmental chemistry.*, 88 (1) : 35.

Cantau. C, Pigot. T, Dupin. J. C and Lacombe. S 2010. N-doped TiO_2 by low temperature synthesis: stability photo-reactivity and singlet oxygen formation in the visible range. *J. Photochemistry and PhotobiologyA: Chemistry.,* 216 (2-3): 201- 208.

Chang. M .S, C. Y. Hou, P. H. Lo and C.T. Chan. 2009. , Preparation of phosphate Zr-doped TiO2 exhibiting high photocatalytic activity through calcinations of ligand-capped nanocrystals. *Applied catalysis B:Environmental.*, 90 :233-241.

Chen. C. C 2007. Degradation pathways of ethyl violet by photocatalytic reaction with ZnO Dispersions. *Journal of Molecular Catalysis. A: Chemical.,* 264: 82-92.

Chiou. H. C and Juang.S. R. 2007. Photocatalytic degradation of phenol in aqueous solutions by Pr-doped TiO_2 nanoparticles. *Journal of Hazardous Materials*: B., 149: 669-678.

Choi. W, Termin. A and Hoffmann. M. R. 1994. The Role of Metal Ion Dopants in Quantum-Sized TiO_2: Correlation between Photoreactivity and Charge Carrier Recombination Dynamics. *Journal of Physical Chemistry.,* (98): 13669-13679.

Elmorsi. M. T, Y. M. Riyad. M. Y. T, Mohamed. H. Z and Bary. E. A. H. M. 2010. De-colorization of Mordant red 73 azo dye in water using H2O2/ UV and photo-Fenton treatment. *Journal of Hazardous Materials*., 174: 352–358.

Fan. X. X, Wang. V. T, Zhgng. J, Gao. I, Li. S. Z, Ye. H. J and Zou. G. Z. 2008. Role of phosphorus in synthesis of phosphate mesoporus TiO_2 photocatalytic materials by EISA method. *Applied Surface Science*., 254:5191-5198.

Gomathi Devi. L, Murthy. N. B and Kumar. G. S. 2010. Photocatalytic activity of TiO_2 doped with Zn^{2+} and V^{5+}transition metal ions: Influence of crystallite size and dopant electronic configuration on photocatalytic activity. *Materials Science and Engineering*: B ., 166 (1) : 1-6.

Huang. D, Liao. S, Quan. S, Liu. L, He. Z, Wan. J and Zhou. W . 2007. Preparation of anatase F doped TiO2 sol and its performance for photodegradation of formaldehyde. *Journal of Materials Science.,* 42: 8193-8202.

Kapusuz. D, Park. J , Ozturk. A. 2013. Sol–gel synthesis and photocatalytic activity of B and Zr co-doped TiO_2 . *Journal of Physics and Chemistry of Solids.,*74 (7) : 1026–1031.

Kapusuz. D, Park. J and Ozturk. A. 2011. Influence of Boron and/or Zirconium doping on morphology and optical properties of Ttania. *Nanocon* ., 21:21–23.

Kim. W. S, Khan. R, T. J. Kim. J. T and Kim. J. W. 2008. Synthesis, characterization and application of Zr,S Co-doped TiO2 as visible-light active photocatalyst. *Bulletin of the Korean Chemical Society*., 29: 1217–1223.

Kusvuran. E, Gulnaz. O, Irmak. S, Atanur. M. O, Yavuz. I. H and Erbatur. O. 2004. Comparison of several advanced oxidation processes for the decolourization of Reactive Red 120 azo dye in aqueous solution. *Journal of Hazardous Materials: B*., 109: 85-93.

Lachheb. H, Eric. P, Houas. A, Mohemed. K, Elaloui. E, Guillard. C and Herrmann. M. J. 2002. Photocatalytic degradation of various types of dyes (Alizarin S, Crocein Orange G, Methyl Red, Congo Red, Methylene

Blue) in water by UV-irradiated titania. *Applied Catalysis B: Environmental.*, 39 (1): 75–90.

Lin. L, W. Lin. W, Xie. L. J, Zhue. X. Y, B. Y. Zhao. Y. B and Y. C. Xie. B. Y. 2007. Photocatalytic properties of phosphor-doped titania nanoparticles. *Applied catalysis B: Environmental* ., 75: 52-58.

Liu. X, Z. Liu. Z, Zheng. J, Yan. X, Li. D, Chen . S and Chu. W. 2011. Characteristics of N- doped TiO_2 nano tube arrays by N_2–Plasma for visible light driven photocatalysis. *Journal of Alloys and compounds*., 509: 9970-9976.

Lv. Y, Yu. L, Huang, H, Liu. H and Feng. Y. 2009. Preparation, Characterization of P-doped TiO_2 nanoparticles and their excellent photocatalytic properties under the solar light irradiation. *Journal of Alloys and Compounds.,* 488 (1) : 314-319.

Ma. J. L and Guo. J. L. 2011. Study of the phase transformation of TiO2 with in situ XRD in different gas. *Spectroscopic analysis Applied surface science .,* 289: 306-315.

Meshesha. S. D, Ravi Chandra. M, Siva Rao. T and Sreedhar. B. 2017 Synthesis and characterization of $Ba^{2+}$and Zr^{4+} co-doped titania nanomaterial which in turn used as an efficient photocatalyst for the degradation of rhodamine-B in visible light. *South african journal of chemical engineering*., 23: 10-16.

Mittal. A, D. Kaur. D and Mittal. D. 2009. Batch and bulk removal of a triarylmethane dye, Fast Green FCF, from waste water by adsorption over waste materials. *Journal of Hazardous materials.,* 163 (2-3) : 567-577.

Mugundan. S, Rajamannan. B, Viruthagiri. G, Shanmugam. N, Gobi. R and Praveen. P. 2015. Synthesis and characteration of undoped and cobalt-doped TiO_2 nanoparticles via sol-gel technique. *Applied Nanoscience* ., 5: 449-456.

Najibi. H, Amir. H. M and B. Tohidi. B. 2006. Estimating the hydrate safety margin in the presence of salt and/or organic inhibitor using freezing point depression data of aqueous solutions. *Industrial and engineering chemistry research.,* 45*:* 4441- 4446.

Neeruganti. O. Gopal, Hsin-Hsi Lo, Tzu-Feng Ke, Chin-Hua Lee, Chang-Chin Chou, Jyun-De Wu, Shiann-Cherng Shiann-Cherng Sheu and Shyue-Chu Ke. 2012. Visible light active phosphorus doped TiO2 nanoparticles: an EPR evidence for the enhanced charge separation. *The Journal of Physical chemistry C* .,10: 1021-21346 .

Ohno. T, Akiyoshi. M, Umebayashi. T, K. Asai. K, T. Mitsui. T and Matsumura. M. 2004. Preparation of S-doped TiO_2 photocatalysts and their photocatalytic activities under visible light. *Applied Catalysis A: General*., 265(1):115-121.

Putz. M. A, Wang. K, Len. A, Plocek. J, Bezdicka. Khamova. V. T. K. P. G, Ianăşi. C, Săcărescu. L, Mitróová. Z, C. Savii. C, Yan. M and Almásy. L. 2017. Mesoporous silica obtained with methyl triethoxy silane as co-precursor in alkaline medium. *Applied Surface Science*., 424: 275-281.

Rauf. A. M, Meetani. A. M and Hisaindee. S. 2011. An overview on the photocatalytic degradation of azo dyes in the presence of TiO2 doped with selective transition metals. *Desalination.,* 276 : 13-27.

Sharopri. N, and Sud. D. 2015. Ultrasound-assisted synthesis and characterization of visible light responsive nitrogen-doped TiO2 nanomaterials for removal of 2-Chlorophenol. *Desalination and Water Treatment*., 1-13.

Shi. Q, Yang. D, Jiang. Y. Z and Li. J. 2006. Visible-light photocatalytic regeneration of NADH using P-doped TiO2 nanoparticles. *Journal of molecular catalysis* B: Enzyme ., 43: 44-48.

Singla. P, Sharma. M, Pandey. P. O and K. Singh. K. 2014. Photocatalytic degradation of azo dyes using Zn-doped and undoped TiO_2 nanoparticles. *Applied Physics*: A ., 116: 371-378.

Sires. I, Guivarch. E, Oturan. N, Oturan. A. M. 2008. Efficient removal of triphenylmethane dyes from aqueous medium by in situ electrogenerated Fenton's reagent at carbon –felt cathode. *Chemosphere*.,72: 592-600.

Susmitha. T, Siva Rao .T and Sreedhar. B. 2014. Effective catalytic performance of manganese and phosphorus codoped titania nanocatalyst for Orange-II dye degradation under visible light irradiation. *Journal of Environmental Chemical Engineering*., 2:1506-1513.

Tahir. H, Hammed. U, Zanhanzed. Q and Sultan. M 2008. Removal of fast green dye (C.I. 42053) from an aqueous solution using Azadirachta indica leaf powder as a low-cost adsorbent. *African Journal of Biotechnology*., 7 (21): 3906-3911.

Wang. Z, Chem. C, Wu. F, Zou. B, Zha. M, Wang. J and Feng. 2009. Photodegradation of rhodamin B under light by bimetal codoped TiO2 nanocrystals. *Journal of Hazardous Materials.,* 164: 615-620.

Wu. J. C. S and Chen. H. C. 2004. A visible-light response vanadium-doped titania nanocatalyst by sol–gel method. *Journal of Photochemistry and Photobiology. A: Chemistry.,* 163 (3): 509-515.

Wu. W. X, Wu. J. D and Liu. J. X. 2009. Optical investigation on sulphur-doping effects in titanium dioxide nanoparticles. *Applied Physics A: Materials science and Processing*., 97 : 243- 248.

Ya. H. F. 2007. Phase development and photocatalytic ability of gel-derived P-doped TiO_2. *Journal of Materials Research.,* 22: 2565-2572.

Yoong. S. L, F. K. Chong. K. F and Dutta. K. B. 2009. Development of copper-doped TiO2 photocatalyst for hydrogen production under visible light. *Energy*., 34: 1652-1661.

Yu. C, Yu. J and Zhou. W. 2010. WO3 coupled P-TiO2 photocatalyst with mesoporous structure. *Catalysis Letterature* ., 140: 172-183.

Yu. C. J, Ho. W, Yu. J, Yip. H, Wong. K. P and Zhao. J. 2005. Efficient Visible-Light-Induced Photocatalytic Disinfection on Sulfur-Doped Nanocrystalline Titania. *Journal of Environmental science and Technology*., 39: 1175.

Yu. C. J, Zhang. L, Zhang. Z and Zhao. J. 2003. Synthesis and characterization of phosphate mesoporous titanium dioxide with high photocatalytic activity. *Chemical Material.*, 15: 3280-2286.

Yu. F. H and Yu. 2007. Photocatalytic abilities of gel-derived P-doped TiO2. *Journal of physical and chemical solids*., 68:600-607.

Yu. F. H and Yang. T. S 2010. Enhancing thermol stebility and photocatalytic activity anatase-TiO_2 nanoparticles

by co-doping P and Si elements. *Journal of Alloy and Compounds*. 492: 695-700.

Yue. X, Yinshan. J, Li. F, Xia. M, Xuee. B and Li. Y. 2014. Effect of calcined atmosphere on the photocatalytic activity of P-doped TiO2. *Applied surface science*., 289: 306-315.

Zhang. C, Chen. S, Mo. L, Y. Huang. Y, Tian. H, Hu. L, Huo. Z, Dai. S, Kong. F and Pan. X 2011. Charge Recombination and Band-Edge Shift in the Dye-Sensitized Mg^{2+}-Doped TiO2 Solar Cells. *Journal of Physical Chemistry C* .,115 (33):16418-16424.

Zhao.Y, X. Qiu. X and Burda. C. 2008. The Effects of Sintering on the Photocatalytic Activity of N-Doped TiO2 Nanoparticles. *Chemistry of Materials*., 20 (8): 2629-2636.

Zheng. R, Guo. Y, Jin.C, Xie. J, Zhu. J and Xie. Y 2010. Noval thermally stable phosphorus-doped TiO2 photocatalyst synthesized by hydrolysis of Ticl4. *Journal of molecular catalysis A: Chemical*., 319: 46-51.

How to cite this article:

Mulupuri Ravi Kumar *et al* (2018) 'Effects of Phosphorus And Cobalt Co-Doped Anatase Titania on the Degradation of Orange Ii and Antibacterial Activity of Staphylococcus Aureus & Salmonella Typhi in Visible Light', *International Journal of Current Advanced Research,* 07(5), pp. 13015-13024. DOI: http://dx.doi.org/10.24327/ijcar.2018.13024.2310

****